Acta Crystallographica Section F
Structural Biology and Crystallization Communications
ISSN 1744-3091

Expression, purification and preliminary crystallographic analysis of the T6SS effector protein Tse3 from *Pseudomonas aeruginosa*

Defen Lu,[a] Guijun Shang,[a] Qian Yu,[a] Heqiao Zhang,[b] Yanyu Zhao,[a] Huaixing Cang,[b] Lichuan Gu,[a] Sujuan Xu[a] and Yan Huang[a]*

[a]State Key Laboratory of Microbial Technology, Shandong University, Jinan 250100, People's Republic of China, and [b]Institute of Biophysics, Chinese Academy of Sciences, Beijing 100101, People's Republic of China

Correspondence e-mail: huangyan@sdu.edu.cn

Received 4 February 2013
Accepted 14 March 2013

Pseudomonas aeruginosa uses the type VI secretion system (T6SS) to inject effector proteins into rival cells in niche competition. Tse3, one of the effectors of T6SS, is delivered into the periplasm of recipient cells. Tse3 functions as a muramidase that degrades the β-1,4-linkage between *N*-acetylmuramic acid (MurNAc) and *N*-acetylglucosamine (GlcNAc) in peptidoglycan, thus leading to lysis of the recipient cells and providing a competitive advantage to the donor cells. Here, the preliminary crystallographic study of Tse3 is reported. A crystal of Tse3 diffracted to 1.5 Å resolution. It belonged to space group *C*121, with unit-cell parameters a = 166.99, b = 70.13, c = 41.94 Å, α = 90.00, β = 90.52, γ = 90.00° and one molecule per asymmetric unit.

1. Introduction

Recently, the type VI secretion system (T6SS) of Gram-negative bacteria has been demonstrated to deliver effectors into host cells (eukaryotic and prokaryotic) through cell contact (Jani & Cotter, 2010; Hood *et al.*, 2010; Russell *et al.*, 2011; Schwarz *et al.*, 2010). The effectors that are exported by the T6SS are involved in many pathogenic and physiological processes, such as cytoskeleton modification of host cells, escape from predators, biofilm formation and interbacterial competition (Holland, 2010; Cascales, 2008; Hood *et al.*, 2010; Pukatzki *et al.*, 2007; MacIntyre *et al.*, 2010; Russell *et al.*, 2011; Ma & Mekalanos, 2010). Although information has accumulated about this secretion system, its mechanism remains little understood (Gerlach & Hensel, 2007; Filloux *et al.*, 2008).

The basic secretion machine is constructed of 13 'core' proteins which form an envelope-crossing tool and is essential for transport of the effectors (Cascales, 2008). 20–25% of genome-sequenced bacteria possesses T6SSs and some have several T6SSs (Bingle *et al.*, 2008; Boyer *et al.*, 2009). The structures of these T6SS components have revealed that some of them are homologues of the contractile phage tail. The proteins Hcp and VgrG are two structural components. They are secreted by T6SS and can be detected in the culture supernatant (Filloux, 2009; Cascales, 2008). The hexameric ring of Hcp resembles the gp19 protein of bacteriophage T4, which is a phage-tail tube protein. A syringe-like structure formed by three VgrG proteins is homologous to the T4 phage spike complex (Pukatzki *et al.*, 2007; Leiman *et al.*, 2009; Pell *et al.*, 2009). Together, these two proteins constitute a tubular structure with Hcp at the bottom and VgrG at the top. This inverted bacteriophage-like tubular structure injects effectors into rival cells. In this regard, the procedure of target-cell recognition and effector transportation of T6SS is considered to be similar to that envisioned for the bacteriophage (Kanamaru, 2009).

Pseudomonas aeruginosa is a common pathogen in chronically infected cystic fibrosis patients. There are at least three gene clusters in the *P. aeruginosa* genome that encode T6SS components named H1-T6SS [haemolysin co-regulated protein secretion island I (HSI-I)-encoded T6SS] to H3-T6SS (Mougous *et al.*, 2006; Filloux *et al.*, 2008; Hood *et al.*, 2010). The VgrGs are regarded as structural components of T6SS rather than effectors, although they are secreted into the milieu or host cells and some of them with C-terminal domains may interfere with the cytoskeleton of the host cells (Pukatzki *et al.*, 2007; Ma *et al.*, 2009). Recently, three effectors controlled by H1-T6SS in *P. aeruginosa* have been identified and named Tse1–Tse3 (type VI

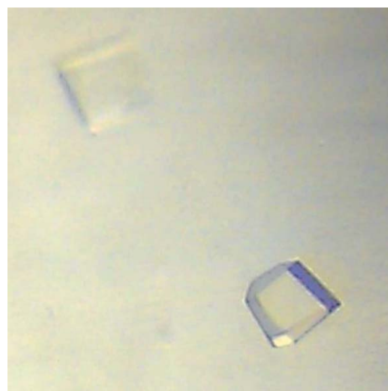

© 2013 International Union of Crystallography
All rights reserved

Table 1
X-ray diffraction data-collection and processing statistics for Tse3.

Values in parentheses are for the outermost shell.

Wavelength (Å)	0.9790
Space group	*C*121
Molecules in asymmetric unit	1
Unit-cell parameters (Å, °)	a = 166.99, b = 70.13, c = 41.94, $\alpha = \gamma$ = 90.00, β = 90.52
Resolution (Å)	50–1.50 (1.54–1.50)
Total No. of reflections	77219
No. of unique reflections	20320
Completeness (%)	98.0 (96.6)
Multiplicity	3.8 (3.7)
$\langle I/\sigma(I)\rangle$	39.9 (4.43)
$R_{\rm merge}$ (%)†	4.8 (33.2)

† $R_{\rm merge} = \sum_{hkl}\sum_i |I_i(hkl) - \langle I(hkl)\rangle| / \sum_{hkl}\sum_i I_i(hkl)$ over i observations.

secretion exported 1–3; Hood *et al.*, 2010; Mougous *et al.*, 2006). Tse2 is delivered into the cytoplasm of rival cells and induces stasis by an unknown mechanism. Tse1 and Tse3, which are released into the periplasm of rival cells, induce the degradation of peptidoglycan, thus leading to lysis of the rival bacteria (Russell *et al.*, 2011). At the same time, *P. aeruginosa* utilizes cognate immunity proteins located in its periplasm to prevent intercellular self-targeting. T6SS immunity 1 (Tsi1) and T6SS immunity 3 (Tsi3) antagonize Tse1 and Tse3, respectively. These three effectors have been shown to endow *P. aeruginosa* with a great advantage during niche competition (Russell *et al.*, 2011).

Tse1 is an amidase that hydrolyzes the γ-D-glutamyl-*meso*-2,6-diaminopimelic acid (D-Glu-mDAP) bond and Tse3 is a muramidase that cleaves the β-1,4-linkage between *N*-acetylmuramic acid (MurNAc) and *N*-acetylglucosamine (GlcNAc) (Russell *et al.*, 2011). Besides Tse1, there are also various type VI amidase effector (Tae) proteins which employ amidases with various bond specificities to cut the peptide chain of the peptidoglyan at different sites (Russell *et al.*, 2012). To date, structures of Tse1, the Tse1–Tsi1 complex and Tsi2 have been solved (Ding *et al.*, 2012; Benz *et al.*, 2012; Shang *et al.*, 2012; Li *et al.*, 2012; Zou *et al.*, 2012). The crystal structures of Tse1 and the Tse1–Tsi1 complex revealed that Tse1 is a novel amidase with a catalytic dyad and that the interaction between Tse1 and Tsi1 is highly specific and strong (Shang *et al.*, 2012). The crystal structure of Tsi2 revealed that it functions as a stable dimer (Zou *et al.*, 2012; Li *et al.*, 2012). However, structures of Tse3 and the Tse3–Tsi3 complex are not available. In this paper, we report the expression, purification and preliminary crystallographic analysis of Tse3.

2. Methods and materials

2.1. Molecular cloning

The gene encoding the fragment Tse3$^{1–402}$ (the UniProt accession code for Tse3 is Q9HYC5) was PCR-amplified from *P. aeruginosa* PAO1 genomic DNA using *Pfu* DNA polymerase. The forword oligonucleotide primer was 5′-GAAATTC**CATATG**ACCGCCAC-CAAGCGAC-3′ and the reverse oligonucleotide primer was 5′-TTT**CTCGAG**GTCGAGGAAGGTGGCGTAG-3′. *Nde*I and *Xho*I restriction-enzyme recognition sites (bold) were added to the forward primer and the reverse primer, respectively. The Tse3$^{1–402}$ fragment was cloned into the pET-21b(+) vector, resulting in the pET-21b-Tse3$^{1–402}$ plasmid encoding a C-terminally His_6-tagged sequence. The construction was verified by sequencing and the pET-21b-Tse3$^{1–402}$ plasmid was transformed into *Escherichia coli* strain BL21 (DE3) for protein expression.

2.2. Protein expression and purification

E. coli BL21 (DE3) cells containing the pET-21b-Tse3$^{1–402}$ plasmid were grown in Luria broth (LB) medium with 100 µg ml^{-1} ampicillin. IPTG was added to a final concentration of 0.1 m*M* to induce protein expression when the OD_{600} reached 0.6, and the temperature was decreased to 289 K. The cells were collected by centrifugation (30 min, 12 000*g*) about 16 h later. The cells were resuspended in buffer *A* (20 m*M* Tris–HCl pH 7.5, 500 m*M* NaCl) and lysed by sonication. The supernatant obtained by centrifugation at 30 000*g* for 45 min was applied onto an Ni-chelating Sepharose (GE Healthcare) affinity column pre-equilibrated with buffer *A*. The affinity column was washed with buffer *B* (20 m*M* Tris–HCl buffer pH 7.5, 500 m*M* NaCl, 10 m*M* imidazole). Tse3$^{1–402}$ was eluted with buffer *C* (20 m*M* Tris–HCl buffer pH 7.5, 500 m*M* NaCl, 200 m*M* imidazole). Finally, Tse3$^{1–402}$ was purified using a Superdex 200 size-exclusion column (GE Healthcare) in buffer *D* (10 m*M* Tris–HCl pH 7.5, 300 m*M* NaCl). The fractions containing purified Tse3$^{1–402}$ were collected according to the protein purity as examined by SDS–PAGE; the final protein concentration for crystallization was 8 mg ml^{-1}.

2.3. Crystallization and optimization

Crystals of Tse3$^{1–402}$ were obtained at 293 K by the sitting-drop vapour-diffusion method. Tse3$^{1–402}$ (8 mg ml^{-1}) was crystallized by mixing equal volumes (1 µl each) of protein solution and reservoir solution consisting of 0.05 *M* $CaCl_2$, 0.05 *M* $NiCl_2$, 0.05 *M* $CdCl_2$, 15%(*w*/*v*) PEG 3350. The initial crystals of Tse3$^{1–402}$ appeared as multiple crystals that were not suitable for diffraction. The streak-seeding method (Bergfors, 2003; Zhu *et al.*, 2005) was employed to optimize the crystals. To prepare a microseed stock, the initial crystals were pulverized using a glass rod and diluted into 1 ml stabilizing

```
Conf:
Pred:
Pred: EEEEEEEHHHHHHHCCCCHHHCCCCHHHHHHHHCCCHHHH
  AA: VVVSTAIKYELFTDLLGQPVRRGLSRKAVATLLASDEFNI
                    290       300       310       320

Conf:
Pred:
Pred: HHHHHHHHHHHHHHHHHHHHHHCCCCCCCCCCCCCCCCCC
  AA: FATARYIRYVANLASQQDLRKLPKTRGAFPSIDLRAYAGN
                    330       340       350       360

Conf:
Pred:
Pred: CCCCCCHHHHHHHHHHCCCCCCCCCCCCCCHHHHHHHHHH
  AA: PRNWPRDNVRALASEYTSRPWDDNLSPGWPMFVDDAYATF
                    370       380       390       400

Conf:
Pred:
Pred: CCCCCCCC
  AA: LDPGMRFP
```

Figure 1
Secondary-structure prediction based on the sequence of Tse3 (only the C-terminal part is shown) using the *PSIPRED* server. C, coil (represented by black lines); H, α-helix (represented by pink tubes); E, β-sheet (represented by yellow arrows). Conf, confidence of prediction (higher confidence is indicated by increased height and colour intensity of the rectangles). Pred, predicted secondary structure. AA, targeted sequence. The deleted sequence is indicated in a green box.

stock buffer [0.05 *M* $CaCl_2$, 0.05 *M* $NiCl_2$, 0.05 *M* $CdCl_2$, 17%(*w*/*v*) PEG 3350]. A cat whisker was dipped into the microseed stock to pick up seeds and was then streaked across a series of new drops. 4 d later, large single Tse3$^{1–402}$ crystals with average dimensions of 0.07 × 0.15 × 0.15 mm that were suitable for diffraction appeared in the drops.

2.4. Data collection and processing

Crystal diffraction data were collected using a MAR345 CCD detector at a crystal-to-detector distance of 200 mm on beamline BL17U1 at Shanghai Synchrotron Radiation facility (SSRF), Shanghai, People's Republic of China. The crystal was rotated through 180° with 1° oscillation and 1 s exposure per frame. In order to prevent radiation damage, the crystals were flash-cooled in a nitrogen stream at 100 K in the presence of reservoir buffer containing 15%(*v*/*v*) glycerol. The data collected were indexed, integrated and scaled with *HKL*-2000 (Otwinowski & Minor, 1997). Data-collection statistics are listed in Table 1.

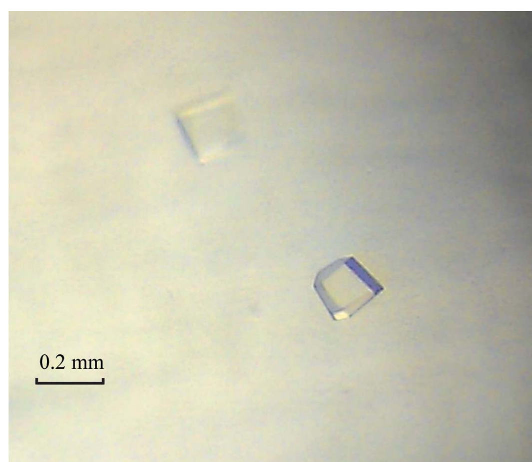

Figure 2
Typical crystals of Tse3$^{1–402}$. The crystals were grown in 0.05 *M* $CaCl_2$, 0.05 *M* $NiCl_2$, 0.05 *M* $CdCl_2$, 15%(*w*/*v*) PEG 3350 using the sitting-drop vapour-diffusion method at 293 K after streak-seeding. These crystals reached average dimensions of 0.07 × 0.15 × 0.15 mm after 4 d.

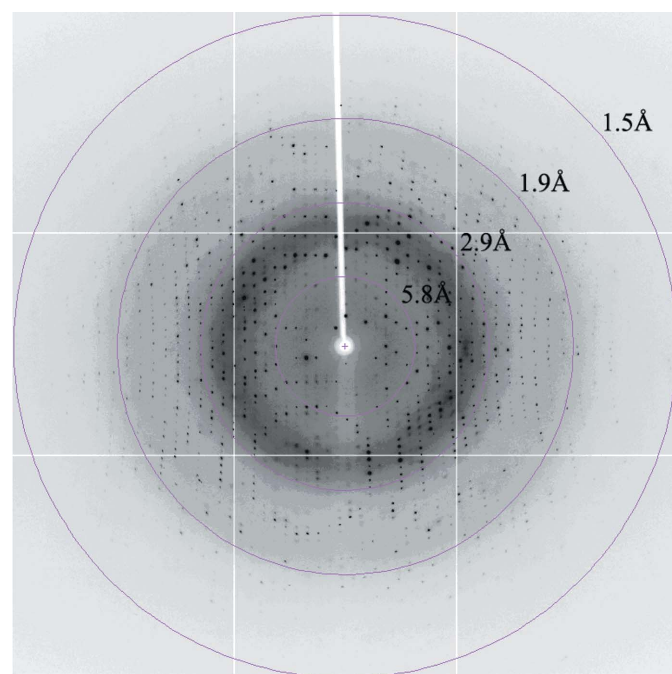

Figure 3
Diffraction pattern of Tse3$^{1–402}$ collected using a MAR345 CCD detector on the BL17U1 beamline at SSRF. The resolution rings are shown as violet circles. The data collected were processed to 1.5 Å resolution.

3. Results and discussion

Full-length Tse3$^{1–408}$ was purified and screened for crystallization. However, no hits were found. Secondary-structure prediction using the *PSIPRED* server (Jones, 1999) indicated that the six residues at the C-terminus of Tse3 do not appear to form secondary structure, which probably hinders the crystallization of Tse3 (Fig. 1). Therefore, the six residues at the C-terminus were deleted in an alternative construct while the catalytic domain was kept intact. The Tse3$^{1–402}$ fragment was inserted into the expression vector pET-21b(+) between the *Nde*I and *Xho*I restriction sites and eight extra residues (LEHHHHHH) were added to the protein, which had a molecular weight of 44.77 kDa and a theoretical pI of 7.80. Fortunately, this fragment crystallized. The crystallization condition was 0.05 *M* $CaCl_2$, 0.05 *M* $NiCl_2$, 0.05 *M* $CdCl_2$, 15%(*w*/*v*) PEG 3350. The crystals were optimized using streak-seeding (Fig. 2). 15%(*v*/*v*) glycerol was used as a cryoprotectant. The crystal diffracted to 1.5 Å resolution (Fig. 3) and belonged to space group *C*121, with unit-cell parameters $a = 166.99$, $b = 70.13$, $c = 41.94$ Å, $\alpha = 90.00$, $\beta = 90.52$, $\gamma = 90.00°$. The solvent content was about 53.82%, with a corresponding Matthews coefficient (Matthews, 1968) of 2.66 $Å^3\,Da^{-1}$ and one molecule per asymmetric unit. Since Tse3 is a member of the G-type lysozyme family (Russell *et al.*, 2011), we attempted to solve the structure of Tse3 by the molecular-replacement method using the coordinates of goose egg-white lysozyme (GEWL; PDB entry 154l; Weaver *et al.*, 1995) as the search model. However, the program *Phaser* (McCoy *et al.*, 2007) gave no correct solution, indicating different conformations of the two molecules. Crystals of an SeMet derivative of Tse3$^{1–402}$ have been obtained. The structure of Tse3 will be solved using either the single-wavelength or the multiple-wavelength anomalous diffraction (SAD or MAD) method (Terwilliger, 2003).

We thank the staff of beamline BL17U1 at Shanghai Synchrotron Radiation Facility for support during data collection. This work was supported by the State Key Laboratory of Microbial Technology, Shandong University, the Hi-Tech Research and Development Program of China (grant No. 2006AA02A324) and the Natural Science Foundation of Shandong Province, China (grant No. ZR2012CQ006).

References

Benz, J., Sendlmeier, C., Barends, T. R. & Meinhart, A. (2012). *PLoS One*, **7**, e40453.
Bergfors, T. (2003). *J. Struct. Biol.* **142**, 66–76.
Bingle, L. E., Bailey, C. M. & Pallen, M. J. (2008). *Curr. Opin. Microbiol.* **11**, 3–8.
Boyer, F., Fichant, G., Berthod, J., Vandenbrouck, Y. & Attree, I. (2009). *BMC Genomics*, **10**, 104.
Cascales, E. (2008). *EMBO Rep.* **9**, 735–741.
Ding, J., Wang, W., Feng, H., Zhang, Y. & Wang, D.-C. (2012). *J. Biol. Chem.* **287**, 26911–26920.
Filloux, A. (2009). *EMBO J.* **28**, 309–310.
Filloux, A., Hachani, A. & Bleves, S. (2008). *Microbiology*, **154**, 1570–1583.
Gerlach, R. G. & Hensel, M. (2007). *Int. J. Med. Microbiol.* **297**, 401–415.
Holland, I. B. (2010). *Methods Mol. Biol.* **619**, 1–20.
Hood, R. D. *et al.* (2010). *Cell Host Microbe*, **7**, 25–37.

Jani, A. J. & Cotter, P. A. (2010). *Cell Host Microbe*, **8**, 2–6.
Jones, D. T. (1999). *J. Mol. Biol.* **292**, 195–202.
Kanamaru, S. (2009). *Proc. Natl Acad. Sci. USA*, **106**, 4067–4068.
Leiman, P. G., Basler, M., Ramagopal, U. A., Bonanno, J. B., Sauder, J. M., Pukatzki, S., Burley, S. K., Almo, S. C. & Mekalanos, J. J. (2009). *Proc. Natl Acad. Sci. USA*, **106**, 4154–4159.
Li, M., Le Trong, I., Carl, M. A., Larson, E. T., Chou, S., De Leon, J. A., Dove, S. L., Stenkamp, R. E. & Mougous, J. D. (2012). *PLoS Pathog.* **8**, e1002613.
Ma, A. T., McAuley, S., Pukatzki, S. & Mekalanos, J. J. (2009). *Cell Host Microbe*, **5**, 234–243.
Ma, A. T. & Mekalanos, J. J. (2010). *Proc. Natl Acad. Sci. USA*, **107**, 4365–4370.
MacIntyre, D. L., Miyata, S. T., Kitaoka, M. & Pukatzki, S. (2010). *Proc. Natl Acad. Sci. USA*, **107**, 19520–19524.
Matthews, B. W. (1968). *J. Mol. Biol.* **33**, 491–497.
McCoy, A. J., Grosse-Kunstleve, R. W., Adams, P. D., Winn, M. D., Storoni, L. C. & Read, R. J. (2007). *J. Appl. Cryst.* **40**, 658–674.
Mougous, J. D., Cuff, M. E., Raunser, S., Shen, A., Zhou, M., Gifford, C. A., Goodman, A. L., Joachimiak, G., Ordoñez, C. L., Lory, S., Walz, T., Joachimiak, A. & Mekalanos, J. J. (2006). *Science*, **312**, 1526–1530.
Otwinowski, Z. & Minor, W. (1997). *Methods Enzymol.* **276**, 307–326.
Pell, L. G., Kanelis, V., Donaldson, L. W., Howell, P. L. & Davidson, A. R. (2009). *Proc. Natl Acad. Sci. USA*, **106**, 4160–4165.
Pukatzki, S., Ma, A. T., Revel, A. T., Sturtevant, D. & Mekalanos, J. J. (2007). *Proc. Natl Acad. Sci. USA*, **104**, 15508–15513.
Russell, A. B., Hood, R. D., Bui, N. K., LeRoux, M., Vollmer, W. & Mougous, J. D. (2011). *Nature (London)*, **475**, 343–347.
Russell, A. B., Singh, P., Brittnacher, M., Bui, N. K., Hood, R. D., Carl, M. A., Agnello, D. M., Schwarz, S., Goodlett, D. R., Vollmer, W. & Mougous, J. D. (2012). *Cell Host Microbe*, **11**, 538–549.
Schwarz, S., Hood, R. D. & Mougous, J. D. (2010). *Trends Microbiol.* **18**, 531–537.
Shang, G., Liu, X., Lu, D., Zhang, J., Li, N., Zhu, C., Liu, S., Yu, Q., Zhao, Y., Zhang, H., Hu, J., Cang, H., Xu, S. & Gu, L. (2012). *Biochem. J.* **448**, 201–211.
Terwilliger, T. C. (2003). *Methods Enzymol.* **374**, 22–37.
Weaver, L. H., Grütter, M. G. & Matthews, B. W. (1995). *J. Mol. Biol.* **245**, 54–68.
Zhu, D.-Y., Zhu, Y.-Q., Xiang, Y. & Wang, D.-C. (2005). *Acta Cryst.* D**61**, 772–775.
Zou, T., Yao, X., Qin, B., Zhang, M., Cai, L., Shang, W., Svergun, D. I., Wang, M., Cui, S. & Jin, Q. (2012). *J. Mol. Biol.* **417**, 351–361.